Stenoparib, an inhibitor of cellular poly (ADP-ribose) polymerases (PARPs), blocks *in vitro* replication of SARS-CoV-2 variants

Katherine E Zarn[a¶], Sierra A Jaramillo[a¶], Anthony R Zapata[a], Nathan E Stone[a], Ashley N Jones[a], Haley E Nunnally[a], Erik W Settles[ab], Ken Ng[a], Paul S Keim[ab], Steen Knudsen[c], Patricia M Nuijten[d], Aloys SI Tijsma[d], Christopher T French[abe*].

[a] Pathogen and Microbiome Institute, Northern Arizona University, Flagstaff, Arizona, United States of America

[b] Department of Biological Sciences, Northern Arizona University, Flagstaff, Arizona, United States of America

[c] Allarity Therapeutics, DK-2970 Hørsholm, Denmark

[d] Viroclinics-DDL, Rotterdam, The Netherlands

[e] COVID-19 Testing Service Center (CTSC), Pathogen and Microbiome Institute, Northern Arizona University, Flagstaff, Arizona, United States of America

* Corresponding Author

Email: ctfrench@nau.edu

[¶] These authors contributed equally to the study.

Abstract

We recently published a preliminary assessment of the activity of a poly (ADP-ribose) polymerase (PARP) inhibitor, stenoparib, also known as 2X-121, which inhibits viral replication by affecting pathways of the host. Here we show that stenoparib effectively inhibits two SARS-CoV-2 wild-type (wt) strains and four additional variant strains; *alpha* (B.1.1.7), *beta* (B.1.351), *delta* (B.1.617.2) and *gamma* (P.1) *in vitro*, with 50% effective concentration (EC_{50}) estimates of 5.6 μM, 9.6 μM, 50.0 μM, 5.0 μM and 13.1 μM, respectively. A separate experiment focusing on a combination of 10 μM stenoparib and 0.5 μM remdesivir, an antiviral drug, resulted in over 80% inhibition of the *alpha* (B.1.1.7) variant, which is substantially greater than the effect achieved either drug alone, suggesting at least additive effects from combining the different mechanisms of activity of stenoparib and remdesivir.

Introduction

As of February 2022, the coronavirus disease (COVID-19) pandemic, caused by SARS-CoV-2, has caused over 430 million infections and over 5.9 million deaths worldwide [1].
36 Although protective vaccines are available, the pandemic continues and both old and new SARS-CoV-2 variants exhibit varying degrees of resistance to vaccination and disease severity. Additional effective therapeutics are urgently needed. Here we describe the activity of a small molecule, stenoparib, an inhibitor of mammalian poly (ADP-ribose) polymerases (PARPs). We
40 show that stenoparib effectively inhibits replication of SARS-CoV-2 wild-type and variant strains *in vitro*.

SARS-CoV-2 has undergone adaptation and mutation since the beginning of the COVID-19 pandemic, resulting in new variants of the virus. Only two antiviral drugs - remdesivir and
44 molnupiravir, or treatment with monoclonal antibodies, have been approved by the United States Food and Drug Administration as COVID-19 therapies under the Emergency Use Authorization [2, 3]. Remdesivir and molnupiravir are nucleoside analogs that affect the activity of the RNA-dependent RNA polymerase (RdRp). After incorporation into viral RNA, remdesivir
48 stalls the RdRp during elongation [4], while molnupiravir results in the incorporation of mutations that can be functionally deleterious [5].

We recently published a study on the activity of a poly (ADP-ribose) polymerase (PARP) inhibitor, stenoparib, also known as 2X-121, which inhibits viral replication by affecting pathways
52 of the host [6] as opposed to targeting viral replication. ADP-ribosylation (ADPR) pathways may have either anti- or pro-viral properties, and their importance in host-virus interactions is becoming increasingly recognized [7]. Unlike remdesivir, which inhibits viral replication downstream of entry into the cell, stenoparib inhibits virus entry and post-entry processes [6].
56 Stenoparib inhibited the SARS-CoV-2 USA-WA1/2020 virus and the HCoV-NL63 human seasonal respiratory coronavirus *in vitro*, exhibiting dose-dependent suppression of virus multiplication and cell-cell spread in cell culture [6]. Stenoparib exhibits a unique dual activity

against the PARP1, 2 and PARP5a, 5b (tankyrase 1, 2) enzymes, which are important intermediates in the Wnt/β-catenin immune checkpoint [8, 9]. As a host-targeting therapeutic that does not directly select for resistance in viruses, we hypothesize that stenoparib should be able to inhibit all SARS-CoV-2 variant strains.

Materials and Methods

Cell Culture. The antiviral activity of stenoparib on SARS-CoV-2 was assessed *in vitro* using Vero E6 *Cercopithecus aethiops* kidney cells (ATCC® CRL-1586™) maintained in EMEM (Eagle's Minimum Essential Medium; cat # 30-2003, ATCC, Manassas, VA, USA) supplemented with 2% or 10% fetal bovine serum (FBS), 100 U/mL penicillin, 100 µg/mL streptomycin, 0.01 M HEPES buffer solution, 1 mM sodium pyruvate, 1x non-essential amino acids solution (cat # SH3023801, Thermo Fisher Scientific, Waltham, MA, USA).

ViroSpot assay. We explored the activity of stenoparib and remdesivir against the SARS-CoV-2 virus and 4 additional SARS-CoV-2 variants of concern; wild-type strain (wt) and variant strains *alpha*, *beta, delta*, and *gamma* (Table 1). We performed ten, serial 2-fold dilutions of compound, mixed with 100 plaque-forming units (pfu) of virus, and added the mixture to 70% confluent Vero E6 cells growing in multi-well plates. SARS-CoV-2 strains were transferred to Vero E6 cells which were fixed and stained 20 hours (h) after infection with a SARS-CoV/SARS-CoV-2 Nucleocapsid monoclonal antibody (Sino Biological) followed by a horseradish peroxidase (HRP)-labeled Goat anti-Mouse IgG (Thermo Scientific) and TrueBlue substrate. Spots were counted using an ImmunoSpot® Image Analyzer as previously described [10]. The EC_{50} values were approximated using package drc 3.0-1 in R version 4.1.1 [11, 12]. Percent inhibition was normalized by taking the average fraction of the wells that showed positive staining compared to the control wells with the highest positive staining [10].

Plaque assay. Vero E6 (ATCC CRL-1586) cells were infected with the SARS-CoV-2 *alpha* variant using a multiplicity of infection (MOI) of 0.1, and the activity of stenoparib was assessed

with and without remdesivir using a plaque reduction assay. Following viral infection and treatment with stenoparib and/or remdesivir, cells were overlaid with low melting point agarose, fixed at 120 h post infection with 4.0% paraformaldehyde, stained with crystal violet, and plaques were manually counted.

Cytotoxicity Assay. Cytotoxicity was measured using the Promega™ CytoTox 96™ Nonradioactive Cytotoxicity Assay kit (cat # G1780, Promega, Madison, WI, USA) in 50 µL reactions and 96-well format (cat # 161093, Thermo Fisher Scientific, Waltham, MA, USA) according to the manufacturer's protocol. The assay was measured using a BioTeK Synergy™ HT plate reader (model # 7091000, BioTek, Winooski, VT, USA) set at 490 nm wavelength. Vero E6 cells were assessed for cytotoxicity at 5 days post-infection. Percent cytotoxicity was calculated by dividing the experimental LDH release at 490 nm wavelength (OD_{490}) by the maximum LDH release control and multiplying by 100.

Results

We explored the activity of stenoparib against two wt SARS-CoV-2 strains (USA-WA1/2020 and SARS-CoV-2 Germany/BavPat1/2020), and four variant strains; *alpha* (B.1.1.7), *beta* (B.1.351) *delta* (B.1.617.2), and *gamma* (P1), hereafter referred to using Greek nomenclature (Table 1). The *delta* strain carries a deletion in ORF7a and was obtained through BEI Resources, NIAID, NIH: SARS-Related Coronavirus 2, Isolate hCoV-19/USA/PHC658/2021 (Lineage B.1.617.2; Delta Variant, NR-55611, contributed by Dr. Richard Webby and Dr. Anami Patel).

Inhibition of virus replication by stenoparib was dose-dependent, with 50% effective concentration (EC_{50}) estimates ranging between 5.0 µM to 50.0 µM across the 5 virus strains tested (Fig. 1A). Interestingly, the EC_{50} estimate for stenoparib and the *beta* variant (50.0 µM) was 3.8- to 10-fold higher than for the wt, *alpha*, *delta*, and *gamma* variants, which were 5.6 µM,

($p = 7.21\times10^{-7}$); 9.6 μM, ($p = 2.68\times10^{-64}$); 5.0 μM, ($p = 2.20\times10^{-4}$); and 13.1 μM, ($p = 2.56\times10^{-6}$), respectively (S1 Table). An analogous phenomenon was noted for remdesivir and the *beta* variant (Fig. 1B), where the EC_{50} (8.9 μM) was 1.8- to 8.9-fold higher than for the wt, *alpha*, *delta*, and *gamma* variants; 4.6 μM, ($p = 3.79\times10^{-4}$); 4.9 μM, ($p = 3.56\times10^{-8}$); 1.0 μM, ($p = 1.34\times10^{-5}$); and 4.8 μM ($p = 9.82\times10^{-4}$), respectively (S1 Table). The virospot experiment was conducted in quadruplicate and infected and untreated cells were used as controls.

In an additional set of experiments, we focused on the SARS-CoV-2 *alpha* variant. Vero E6 cells were infected with the *alpha* variant using a multiplicity of infection of 0.1, and the activity of stenoparib was assessed with and without remdesivir using the plaque reduction assay. Plaques are areas of dead or destroyed cells and appear as small, clear regions in an infected cell monolayer after fixation and staining with crystal violet. We combined 2.5, 5.0, and 10 μM doses of stenoparib with the previously reported EC_{50} of remdesivir (0.5 μM) [6]. The 3 control types were 1) infected and untreated cells, 2) uninfected and untreated cells, and 3) infected cells treated with a combination of camostat mesylate and E64d (CE), which are protease inhibitors that prevent spike protein cleavage and virus entry into the cell [12].

As shown in Fig. 2A and 2B, neither 10 μM stenoparib nor 0.5 μM remdesivir achieved greater than a 50% reduction in plaquing efficiency compared to the infected, untreated cells. When combined, however, plaque formation was reduced by over 80% compared to infected, untreated cells. This reduction was superior to what was achievable with stenoparib ($p = 3.03\times10^{-5}$) or remdesivir ($p = 1.99\times10^{-4}$) alone at these doses. Notably, cytotoxicity remained near baseline levels (Fig. 2C). The cytotoxicity experiment was run in quadruplicate and cells were treated with CE, dimethylsulfoxide (DMSO), lysis buffer, or left untreated (no compound) as controls. When combined, the activity of two or more drugs with different mechanisms of activity may synergize, with the potential benefit of reducing individual doses of each drug and minimizing undesirable side effects in the patient.

136 **Discussion**

According to a recent report, the *beta* variant appears to exhibit a significantly reduced eclipse period and more rapid replication *in vitro* compared to the *alpha* variant [14], which could explain the relatively higher stenoparib and remdesivir EC_{50} estimates for the *beta* variant. In
140 addition to numerous changes to the Spike (S) protein, the *beta* variant carries some unique mutations in the N protein and in the Nsp3 polyprotein (ORF1a) that are not found in the other variants [15], and may be involved in viral degradation pathways including ADPR following infection [16]. Differential susceptibility to ADPR may be related to the altered replication
144 kinetics of the *beta* variant, although this awaits experimental validation.

Besides the known roles for the PARP1 and PARP2 enzymes in DNA repair [17, 18], members of the PARP family have numerous additional functions [19]. The 18 known human PARPs appear to differentially affect viral replication; some exhibit proviral activity and others
148 exhibit antiviral roles [7, 20-24]. In coronavirus, the N protein is mono (ADP) ribosylated (MARylated) during infection. Stability of the N protein is critical for viral genome replication, translation, packaging, and modulation of the host cell cycle [25]. The N protein is the only ADPR target definitively identified in coronavirus thus far [20], and the prevalence of this
152 modification across multiple coronavirus families suggests an important role in virus stability [20]. Despite this, the role of N protein MARylation, and of ADPR in general with regards to coronavirus stability, is not well characterized. Possibly ADPR has a role in regulating virus genome structure, like ADPR of histones or the adenovirus core proteins [26, 27]. While
156 remdesivir and molnupiravir inhibit viral RNA replication, stenoparib likely acts through multiple targets. A combination of stenoparib and remdesivir or molnupiravir may be highly potent at inhibiting SARS-family coronaviruses including SARS-CoV-2.

A host-targeting therapeutic like stenoparib could be a significant benefit for COVID-19
160 patients as a standalone therapy, or especially as part of a combinatorial COVID-19 treatment strategy with an antiviral drug such as remdesivir or molnupiravir. Combinations of two or more

drugs may lead to synergism through different mechanisms of action, which has the potential benefit of reducing individual doses of each drug and minimizing undesirable side effects.

Acknowledgements

We thank Centers for Disease Control and Prevention, Andrew S. Pekosz, Dr. Richard Webby and Dr. Anami Patel, and National Institute of Infectious Diseases for contributing SARS-CoV-2 variants to facilitate this work.

Author Contributions

Conceptualization: Christopher T. French, Erik W. Settles, Steen Knudsen, Paul Keim

Data curation: Katherine E. Zarn

Formal analysis: Katherine E. Zarn, Christopher T. French, Sierra A. Jaramillo

Funding acquisition: Steen Knudsen, Christopher T. French, Paul Keim

Investigation: Katherine E. Zarn, Sierra A. Jaramillo, Anthony R. Zapata, Ashley Jones, Haley Nunnally, Aloys Tijsma, Patricia Nuijten

Methodology: Christopher T. French, Nathan E. Stone

Project Administration: Christopher T. French, Paul Keim, Steen Knudsen, Aloys Tijsma

Resources: Christopher T. French, Paul Keim

Supervision: Christopher T. French, Erik W. Settles, Paul Keim

Visualization: Ken Ng, Katherine E. Zarn

Writing – Original Draft: Christopher T. French

Writing – Review & Editing: Katherine E. Zarn, Christopher T. French

Competing Interests

SK is employed by and holds a financial interest in Allarity Therapeutics, which stands to potentially benefit from these results.

Funding

188 This research was supported by a grant from The Flinn Foundation, the Cowden Endowment for Microbiology, and an Arizona Board of Regents TRIF award. Core experiments were supported by service fees paid by Allarity Therapeutics.

References

1. WHO. 2021. Available from: https://covid19.who.int/.
2. Prevention USCfDCa. Information for Clinicians on Investigational Therapeutics for Patients with COVID-19 Centers for Disease Control and Prevention: National Center for Immunization and Respiratory Diseases (NCIRD), Division of Viral Diseases; 2020. Available from: https://www.cdc.gov/coronavirus/2019-ncov/hcp/therapeutic-options.html.
3. Beigel JH, Tomashek KM, Dodd LE, Mehta AK, Zingman BS, Kalil AC, et al. Remdesivir for the Treatment of Covid-19 - Final Report. The New England journal of medicine. 2020;383(19):1813-26. Epub 2020/05/24. doi: 10.1056/NEJMoa2007764. PubMed PMID: 32445440; PubMed Central PMCID: PMCPMC7262788.
4. Kokic G, Hillen HS, Tegunov D, Dienemann C, Seitz F, Schmitzova J, et al. Mechanism of SARS-CoV-2 polymerase stalling by remdesivir. Nat Commun. 2021;12(1):279. Epub 2021/01/14. doi: 10.1038/s41467-020-20542-0. PubMed PMID: 33436624; PubMed Central PMCID: PMCPMC7804290.
5. Kabinger F, Stiller C, Schmitzova J, Dienemann C, Kokic G, Hillen HS, et al. Mechanism of molnupiravir-induced SARS-CoV-2 mutagenesis. Nat Struct Mol Biol. 2021;28(9):740-6. Epub 2021/08/13. doi: 10.1038/s41594-021-00651-0. PubMed PMID: 34381216; PubMed Central PMCID: PMCPMC8437801.
6. Stone NE, Jaramillo SA, Jones AN, Vazquez AJ, Martz M, Versluis LM, et al. Stenoparib, an Inhibitor of Cellular Poly(ADP-Ribose) Polymerase, Blocks Replication of the SARS-CoV-2 and HCoV-NL63 Human Coronaviruses In Vitro. mBio. 2021;12(1):e03495-20. doi: 10.1128/mBio.03495-20.
7. Kuny CV, Sullivan CS. Virus-Host Interactions and the ARTD/PARP Family of Enzymes. PLoS pathogens. 2016;12(3):e1005453. Epub 2016/03/25. doi: 10.1371/journal.ppat.1005453. PubMed PMID: 27010460; PubMed Central PMCID: PMCPMC4806868.
8. McGonigle S, Chen Z, Wu J, Chang P, Kolber-Simonds D, Ackermann K, et al. E7449: A dual inhibitor of PARP1/2 and tankyrase1/2 inhibits growth of DNA repair deficient tumors and antagonizes Wnt signaling. Oncotarget. 2015;6(38):41307-23. Epub 2015/10/30. doi: 10.18632/oncotarget.5846. PubMed PMID: 26513298; PubMed Central PMCID: PMCPMC4747407.
9. Thorsell AG, Ekblad T, Karlberg T, Low M, Pinto AF, Tresaugues L, et al. Structural Basis for Potency and Promiscuity in Poly(ADP-ribose) Polymerase (PARP) and Tankyrase Inhibitors. J Med Chem. 2017;60(4):1262-71. Epub 2016/12/22. doi: 10.1021/acs.jmedchem.6b00990. PubMed PMID: 28001384; PubMed Central PMCID: PMCPMC5934274.
10. van Baalen CA, Jeeninga RE, Penders GH, van Gent B, van Beek R, Koopmans MP, et al. ViroSpot microneutralization assay for antigenic characterization of human influenza viruses. Vaccine. 2017;35(1):46-52. Epub 2016/12/03. doi: 10.1016/j.vaccine.2016.11.060. PubMed PMID: 27899226.
11. Ritz C SJ. Package ‘drc’. Analysis of dose-response data is made available through a suite of flexible and versatile model fitting and after-fitting functions. ed. https://cran.r-project.org/web/packages/drc/drc.pdf: CRAN; 2016.
12. Ritz C, Baty F, Streibig JC, Gerhard D. Dose-Response Analysis Using R. PloS one. 2015;10(12):e0146021. Epub 20151230. doi: 10.1371/journal.pone.0146021. PubMed PMID: 26717316; PubMed Central PMCID: PMCPMC4696819.
13. Hoffmann M, Kleine-Weber H, Schroeder S, Kruger N, Herrler T, Erichsen S, et al. SARS-CoV-2 Cell Entry Depends on ACE2 and TMPRSS2 and Is Blocked by a Clinically Proven Protease Inhibitor. Cell. 2020;181(2):271-80 e8. Epub 2020/03/07. doi:

10.1016/j.cell.2020.02.052. PubMed PMID: 32142651; PubMed Central PMCID:
240 PMCPMC7102627.
14. Pyke AT, Nair N, van den Hurk AF, Burtonclay P, Nguyen S, Barcelon J, et al. Replication Kinetics of B.1.351 and B.1.1.7 SARS-CoV-2 Variants of Concern Including Assessment of a B.1.1.7 Mutant Carrying a Defective ORF7a Gene. Viruses. 2021;13(6). Epub
244 2021/07/03. doi: 10.3390/v13061087. PubMed PMID: 34200386; PubMed Central PMCID: PMCPMC8227137.
15. Hodcroft EB. CoVariants: SARS-CoV-2 Mutations and Variants of Interest 2021. Available from: https://covariants.org/.
248 16. Lei J, Kusov Y, Hilgenfeld R. Nsp3 of coronaviruses: Structures and functions of a large multi-domain protein. Antiviral Res. 2018;149:58-74. Epub 2017/11/13. doi: 10.1016/j.antiviral.2017.11.001. PubMed PMID: 29128390; PubMed Central PMCID: PMCPMC7113668.
252 17. Dziadkowiec KN, Gasiorowska E, Nowak-Markwitz E, Jankowska A. PARP inhibitors: review of mechanisms of action and BRCA1/2 mutation targeting. Prz Menopauzalny. 2016;15(4):215-9. doi: 10.5114/pm.2016.65667. PubMed PMID: 28250726; PubMed Central PMCID: PMCPMC5327624.
256 18. Ame JC, Rolli V, Schreiber V, Niedergang C, Apiou F, Decker P, et al. PARP-2, A novel mammalian DNA damage-dependent poly(ADP-ribose) polymerase. The Journal of biological chemistry. 1999;274(25):17860-8. Epub 1999/06/11. doi: 10.1074/jbc.274.25.17860. PubMed PMID: 10364231.
260 19. Gupte R, Liu Z, Kraus WL. PARPs and ADP-ribosylation: recent advances linking molecular functions to biological outcomes. Genes & development. 2017;31(2):101-26. doi: 10.1101/gad.291518.116. PubMed PMID: 28202539.
20. Grunewald ME, Fehr AR, Athmer J, Perlman S. The coronavirus nucleocapsid protein is
264 ADP-ribosylated. Virology. 2018;517:62-8. Epub 2017/12/05. doi: 10.1016/j.virol.2017.11.020. PubMed PMID: 29199039; PubMed Central PMCID: PMCPMC5871557.
21. Grunewald ME, Chen Y, Kuny C, Maejima T, Lease R, Ferraris D, et al. The coronavirus macrodomain is required to prevent PARP-mediated inhibition of virus replication and
268 enhancement of IFN expression. PLoS pathogens. 2019;15(5):e1007756. Epub 2019/05/17. doi: 10.1371/journal.ppat.1007756. PubMed PMID: 31095648; PubMed Central PMCID: PMCPMC6521996.
22. Li L, Zhao H, Liu P, Li C, Quanquin N, Ji X, et al. PARP12 suppresses Zika virus
272 infection through PARP-dependent degradation of NS1 and NS3 viral proteins. Science signaling. 2018;11(535):eaas9332. doi: 10.1126/scisignal.aas9332. PubMed PMID: 29921658.
23. Atasheva S, Frolova EI, Frolov I. Interferon-stimulated poly(ADP-Ribose) polymerases are potent inhibitors of cellular translation and virus replication. Journal of virology.
276 2014;88(4):2116-30. Epub 2013/12/11. doi: 10.1128/JVI.03443-13. PubMed PMID: 24335297.
24. Westera L, Jennings AM, Maamary J, Schwemmle M, Garcia-Sastre A, Bortz E. Poly-ADP Ribosyl Polymerase 1 (PARP1) Regulates Influenza A Virus Polymerase. Adv Virol. 2019;2019:8512363. Epub 2019/04/25. doi: 10.1155/2019/8512363. PubMed PMID: 31015836;
280 PubMed Central PMCID: PMCPMC6444269.
25. McBride R, van Zyl M, Fielding BC. The coronavirus nucleocapsid is a multifunctional protein. Viruses. 2014;6(8):2991-3018. Epub 2014/08/12. doi: 10.3390/v6082991. PubMed PMID: 25105276; PubMed Central PMCID: PMCPMC4147684.
284 26. Déry CV, de Murcia G, Lamarre D, Morin N, Poirier GG, Weber J. Possible role of ADP-ribosylation of adenovirus core proteins in virus infection. Virus Research. 1986;4(4):313-29. doi: https://doi.org/10.1016/0168-1702(86)90078-X.
27. Strickfaden H, McDonald D, Kruhlak MJ, Haince J-F, Th'ng JPH, Rouleau M, et al.
288 Poly(ADP-ribosyl)ation-dependent Transient Chromatin Decondensation and Histone

Displacement following Laser Microirradiation*. Journal of Biological Chemistry. 2016;291(4):1789-802. doi: https://doi.org/10.1074/jbc.M115.694992.

292

Table & Figures

Variant	Pango lineage	Strain	Isolate	Source
Wild type (wt)	-	BavPat1/2020	Germany	European Virus Archive – GLOBAL; 026V-03883
Wild type (wt)	-	USA-WA1/2020	Washington, USA	BEI Resources; NR-52281
alpha	B.1.1.7	hCoV-19/USA/CA_CDC_5574/2020	California, USA	BEI Resources; NR-54011
beta	B.1.351	hCoV-19/USA/MD-HP01542/2021	Maryland, USA	BEI Resources; NR-55282
delta	B.1.617.2	hCoV-19/USA/PHC658/2021	Tennessee, USA	BEI Resources; NR-55611*
gamma	P.1	Isolate hCoV-19/Japan/TY7-503/2021	Japan	BEI Resources; NR-54982

Table 1. SARS-CoV-2 variants tested in Virospot assay to generate dose response curves and estimate EC_{50} values for stenoparib and remdesivir. The wt (USA-WA1/2020) strain was deposited by the Centers for Disease Control and Prevention and obtained through BEI Resources, NIAID, NIH: SARS-Related Coronavirus 2, Isolate USA-WA1/2020, NR-52281. The *alpha* strain was deposited by Centers for Disease Control and Prevention and obtained through BEI Resources, NIAID, NIH: SARS-Related Coronavirus 2, Isolate USA/CA_CDC_5574/2020, NR-54011. The *beta* strain was obtained through BEI Resources, NIAID, NIH: SARS-Related Coronavirus 2, Isolate hCoV-19/USA/MD-HP01542/2021 (Lineage B.1.351), in *Homo sapiens* Lung Adenocarcinoma (Calu-3) Cells, NR-55282, contributed by Andrew S. Pekosz. The *delta* strain carries an ORF7a deletion which may have the potential to impact virulence [14] and was obtained through BEI Resources, NIAID, NIH: SARS-Related Coronavirus 2, Isolate hCoV-19/USA/PHC658/2021 (Lineage B.1.617.2; Delta Variant), NR-55611, contributed by Dr. Richard Webby and Dr. Anami Patel. The *gamma* strain was obtained through BEI Resources, NIAID, NIH: SARS-Related Coronavirus 2, Isolate hCoV-19/Japan/TY7-503/2021 (Brazil P.1), NR-54982, contributed by National Institute of Infectious Diseases.

Fig 1. **Dose-response curves for stenoparib and remdesivir on SARS-CoV-2 variants.**

312 Normalized percent inhibition (Y-axis) of SARS-CoV-2 variants (wild-type (wt): BetaCoV/Munich/BavPat1/2020, European Virus Archive Global. *alpha*: USA/CA_CDC_5574/2020, BEI Resources, Cat# NR-54011. *beta*: hCoV-19/South Africa/KRISP-K005325/2020, BEI Resources. *gamma*: hCoV-19/Japan/TY7-503/2021 (Brazil

316 P.1), BEI Resources) in Vero E6 cells treated with (A) stenoparib and (B) remdesivir at the indicated concentrations (X-axis). Error bars are the standard deviation.

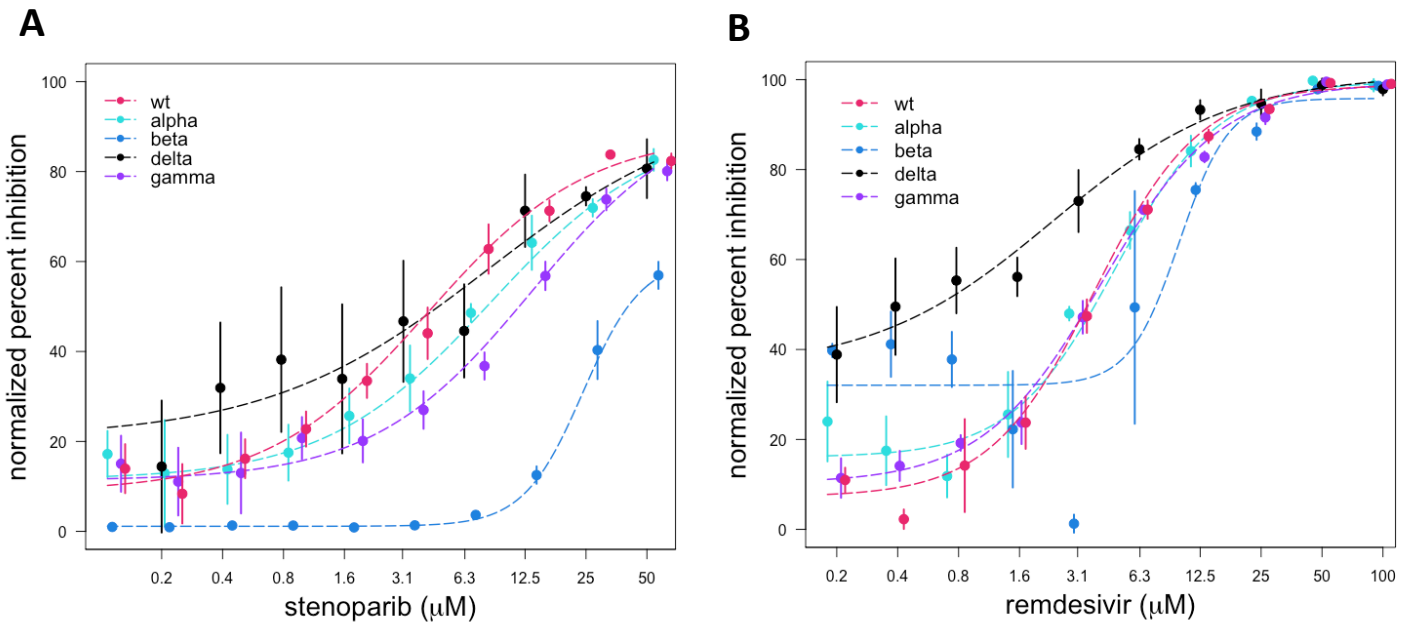

318 **Fig 2.** Activity of stenoparib and remdesivir on the *alpha* (B.1.1.7) variant. (A) Virus Plaque assays. Vero E6 cells (ATCC CRL-1586) were infected for 2 hours with SARS-CoV-2 *alpha* (USA/CA_CDC_5574/2020, BEI Resources, Cat# NR-54011), washed, and overlaid with low-
321 melting temp agarose/MEM with or without stenoparib and/or remdesivir at the concentrations indicated. The cell monolayers were fixed with 4% paraformaldehyde and stained with 0.1% crystal violet prior to manual counting of plaques. The experiment was performed using
324 technical triplicates, and error bars represent the standard deviation of three independent experiments. For pairwise comparisons to untreated cells, * indicates p-values less than 0.05 and ** indicates p-values less than 0.01. (B) Photographs of plate wells after crystal violet
327 staining. Labels indicate the concentrations of stenoparib or remdesivir. Abbreviations; S = stenoparib, R = remdesivir at the concentrations indicated (2.5 / 0.5 = 2.5 μM stenoparib, 0.5 μM remdesivir, etc.). (C) Cytotoxicity measurements performed by the lactate dehydrogenase
330 release assay (Promega Cytotox 96) 48 hours after infection. Inhibitors stenoparib or remdesivir were used at the indicated concentrations (X-axis). The assays were performed according to the manufacturer's recommendations. Results from drug treatments were normalized to the fraction
333 of maximum cytotoxicity (% Cytotoxicity; Y-axis) achieved by detergent lysis of cells. The samples were processed in triplicate, and error bars represent the standard deviation of three independent experiments.

336

339

342

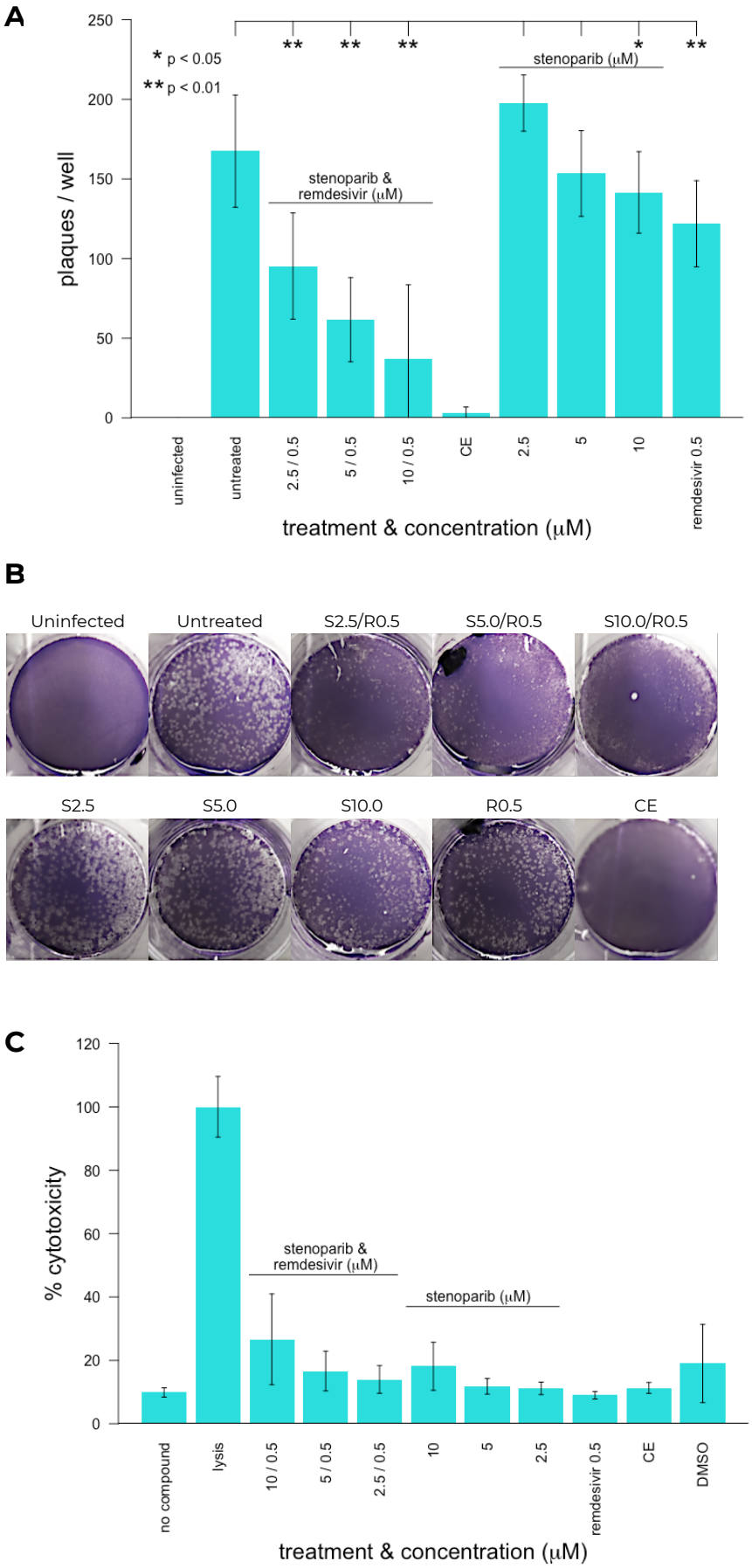
A
* p < 0.05
** p < 0.01
plaques / well
stenoparib & remdesivir (μM)
stenoparib (μM)
uninfected
untreated
2.5 / 0.5
5 / 0.5
10 / 0.5
CE
2.5
5
10
remdesivir 0.5
treatment & concentration (μM)
B
Uninfected
Untreated
S2.5/R0.5
S5.0/R0.5
S10.0/R0.5
S2.5
S5.0
S10.0
R0.5
CE
C
% cytotoxicity
stenoparib & remdesivir (μM)
stenoparib (μM)
no compound
lysis
10 / 0.5
5 / 0.5
2.5 / 0.5
10
5
2.5
remdesivir 0.5
CE
DMSO
treatment & concentration (μM)